XVII[th] World Congress of the International Commission of Agricultural and Biosystems Engineering (CIGR)

Hosted by the Canadian Society for Bioengineering (CSBE/SCGAB)
Québec City, Canada June 13-17, 2010

SHRINKAGE EFFECT ON MOISTURE DIFFUSIVITY CALCULATION DURING SUPERHEATED STEAM DRYING OF DISTILLER'S SPENT GRAIN

MAGDALENA ZIELINSKA[1], STEFAN CENKOWSKI[2]

1 M. Zielinska, m.zielinska@uwm.edu.pl
2 S. Cenkowski, Stefan_Cenkowski@umanitoba.ca

CSBE100664 – Presented at Section VI: Postharvest Technology and Process Engineering Conference

ABSTRACT The aim of this paper was to model the drying kinetics of distiller's spent grain (DSG) on an inert body in superheated steam (SS). The inert material was a Teflon sphere on which a thin layer of DSG was deposited. Drying curves were determined at SS temperatures between 110, 130 and160°C and steam velocity of 1.0 m/s. The falling drying rate data were used to calculate the effective moisture diffusion coefficients from the Fick's equation for an infinite plate of the thickness of the DSG layer deposited on the surface of the inert body. The computer simulations were conducted at the diffusivity determined with no shrinkage and when the change in the layer thickness was due to shrinkage but with the diffusivity determined based on non-shrinkage conditions. Assuming no shrinkage took place, the values of effective moisture diffusivity ranged between 3.02×10^{-8} and 5.28×10^{-8} m^2/s, while it was between 1.45×10^{-9} and 2.06×10^{-9} m^2/s when a change in the layer thickness was due to shrinkage. Neglecting the shrinkage phenomenon during drying overestimated the diffusivity of DSG. The diffusivity coefficient determined for the best fit conditions for the experimental data ranged from 5.08×10^{-10} to 8.24×10^{-10}.

Keywords: Superheated Steam Drying; Distiller's Spent Grain; Drying Modelling; Volume Shrinkage; Effective Moisture Diffusivity.

INTRODUCTION Distiller's spent grain (DSG) is one of the key by-products of ethanol processing, left in distilleries after alcohol is removed by distillation from the fermented grains. It is primarily utilized as a livestock feed ingredient, but it can also be used as a supplement to produce food for human consumption. Due to the massive growth of ethanol industries, a significant production of DSG has occurred over the last several years. The shelf life for distiller's wet grain, with more than 70% moisture content (wet basis), is less than one week. To prolong the storage time of spent grains and to reduce their mass (consequently to lower the transportation cost), spent grains need to be dried. Processing plants typically sell two-thirds of dried distiller's spent grain, but drying can consume 30% of their operating budget. Present trends in drying are associated with higher energy efficiency, enhanced drying rates, system compactness, quality control and optimal capacity. To save energy, typical drying operations that use hot air (HA) can be replaced by superheated steam (SS) as the drying medium (Zielinska et al., 2009).

The main objective of SS drying of DSG is to provide ethanol processors with a substantial revenue source and increase the profitability of the production process. With the present trends in SS drying of liquids, suspensions, slurries, pulps, and pastes; fluidized or spouted bed drying with inert particles has shown a great potential for the production of powders or flakes. In view of the high moisture content of DSG, SS drying could be performed in a fluidized bed of inert particles that provide good conditions for slurry dehydration (Kudra & Mujumdar, 2002). The experiments carried out to date with glass beads, PVC pellets, spherical resin particles, ceramic balls, silica gel spherical particles and teflon cubes and spheres proved that teflon is the most suitable because of no attrition and high capacity to accumulate heat (Benali, 2006). The experiments conducted with teflon spheres of different heat capacity proved that drying of thin-layer DSG on a hollow sphere in comparison to drying on a solid sphere cut the entire drying time by 30% (Zielinska & Cenkowski, 2009).

To improve drying behaviour of DSG in SS a use of mathematical models is promoted. This approach enables simulation of drying under different conditions. The common approach for modeling mass transfer is to use mathematical models considering the concept of the effective diffusivity (D_{eff}), which allows to describe the diffusion of moisture by the Fick's second law (Reyes et al., 2002). The solution of Fick's equation can be applied to different solid geometries, e.g. slab, cylinder and sphere (Crank, 1975). The thin-layer of particulate materials can be defined as a layer of food particles that are being dried and can be modeled by the same drying equations as single food particles suspended in drying medium (Pabis at al., 1998). Then, it can be assumed that the conditions of moisture transfer in the thin-layer of particulate materials on inert body are similar to those observed for an infinite plate dried from one side by the constant SS flow and temperature while the other side of the plate is water-impermeable. For an infinite plate, with the assumptions of moisture migration by diffusion, uniform initial moisture distribution, negligible external resistance to heat and mass transfer, constant temperature, and constant moisture diffusivity from flat material, the solution of Fick's law can be mathematically expressed in the following form (Pabis at al., 1998):

$$MR = \frac{8}{\pi^2}\left[\sum_{n=0}^{\infty}\frac{1}{(2n+1)^2}\exp\left(-\frac{\pi^2(2n+1)^2}{4}\frac{D_{eff}\,t}{s^2}\right)\right] \tag{1}$$

where MR is moisture ratio, D_{eff} is effective moisture diffusivity of the material (m^2/s), s is the thickness of a thin-layer of material to be dried on the inert particle (m), and t is drying time (s). If the infinite plate is suspended in the drying medium, and moisture is removed from only one side of the plate, the parameter s represents the whole thickness of DSG layer on the inert material. To calculate the values of moisture diffusivity of DSG Eqs. (2) and (3) can be applied (Zielinska & Markowski, 2010):

$$D^{i}{}_{eff}\left(T^{i}{}_{m}, M^{i}\right) = \frac{\pi^2 k\left(T^{i}{}_{m}\right)}{4s^2\left(M^{i}\right)}\, i = 1,\ldots,N_s; \tag{2}$$

$$D^{j}{}_{eff} = \frac{\pi^2 k^{j}}{4s^2}\; j = 1,\ldots,N_T \tag{3}$$

where N_s is number of samplings of moisture content of DSG during experiments, N_T is number of SS temperature levels applied during experiments, T_m is material temperature (◦C), M is actual moisture content (kg/kg d.b.), k is constant in Eqs. (2) and (3).

Most of the researchers studying drying of food materials indicate that the moisture content of a particle being dried and temperature of drying medium are two most important factors influencing moisture diffusivity of dried material. However, it is evident that the temperature of drying medium influences the heating rate of dried solid and its moisture diffusivity indirectly. Direct factors affecting the changes in moisture diffusivity of a solid are the parameters of its thermodynamic state, i.e. material temperature and moisture content of the solid. Therefore, an Arrhenius-type equation (4) can be applied after Mulet (1994) to fit the data received from Eqs. (2) and (3):

$$D_{eff} = D_0 \exp\left(-\frac{k_T}{T_m + 273.15} + k_M M \right) \tag{4}$$

where D_0, k_T, k_M are constants.

One of the most important physical changes which occur simultaneously with moisture diffusion is the reduction of external volume of food products. The reduction in volume can affect the heat and mass exchange area, in particular the effective moisture diffusivity of materials, and therefore the overall drying rate. Furthermore, food shrinkage produces a variation in the distance required for the movement of water molecules, making the effective moisture diffusivity overestimated when calculated from analytical solution. The introduction of a volume shrinkage and a parameter which accounts for volume changes when developing the drying models substantially improves their quality (Mulet, 1994). To take shrinkage into consideration the volume of sample at given moisture content can be estimated using the following formula (Mohsenin, 1986):

$$V = \frac{\pi xyz}{6} \tag{5}$$

where x,y,z are orthogonal characteristic dimensions (mm). Changes in volume vs. moisture content of a sample can be described by the linear equation (6):

$$\frac{V}{V_0} = A\frac{M}{M_0} + B \tag{6}$$

where V/V_0 is the volume shrinkage ratio, M/M_0 is the dimensionless moisture ratio, and A, B are coefficients .

Despite numerous published papers on the subject of thin-layer drying of agricultural products, limited information is available on drying of a thin-layer of DSG on an inert material. Therefore, the purpose of the present work was: (i) to identify the effect of SS temperature on drying characteristics of DSG, (ii) to determine the values of the effective moisture diffusivity of DSG and (iii) to show the effect of shrinkage on calculated values of the effective moisture diffusivity of DSG.

MATERIAL AND METHODS Material The work was carried out using stillage (mixture of corn/wheat, 50:50) obtained from a distillery (Mohawk Canada Limited, a division of Husky Oil Limited) in Minnedosa, MB, Canada. The detailed description for sample preparation was given in our previous work (Zielinska et al., 2009). The whole stillage was separated into two fractions: the solid fraction (wet distiller's grain, or distiller's spent grain - DSG) and the liquid fraction containing solubles (thin stillage) After separation, the solid fraction (DSG) was used in drying experiments. A hollow sphere (50.8 mm diameter) made of polytetrafluoroethylene (Virgin Teflon®, PTFE 860;

Applied Plastic Technology Inc., Bristol, RI) served as an inert particle when drying DSG. The hollow sphere was machined from the solid teflon ball that was cut into two hemispheres and the material from the interior was removed leaving a 3.5 mm thick wall. The two hollowed hemispheres were then connected with a metal pin.

Superheated steam drying equipment and procedure The detailed description for the SS processing system and the experimental procedure was given in our previous study (Zielinska et al., 2009). Drying was carried out at SS temperatures of 110, 130 and 160°C and the SS velocity of 1.0. Drying experiments were conducted under atmospheric pressure.

Determination of moisture diffusivity Two general assumptions were made: (a) the moisture diffusivity of DSG depends on material temperature and moisture content, (b) the external resistance to heat and mass transfer is negligible and the surface of the dried DSG is at equilibrium. The moisture diffusivity in DSG during SS drying was determined for the following cases: (i) no shrinkage of DSG during drying, and (ii) the thin layer thickness change due to the shrinkage. The effective diffusivity was determined based on the following procedure: Experimental data were fitted to Eq. (1). Eleven terms in Eq. (1) were used to provide the acceptable accuracy of the results. The volume shrinkage of DSG sample vs. moisture content was calculated from Eq. (6) or was kept constant depending on the equation fitted to the experimental data. To take the shrinkage into consideration, it was assumed that DSG sample did not change their shape during drying but changed their dimensions. Then, the volume shrinkage of DSG during drying with respect to moisture was determined experimentally. Finally, the set of values of moisture diffusivity of DSG for all experimental conditions was calculated from Eqs. (2) and (3).

Volume determination method using image analysis Samples of DSG were shaped into spheres using a kitchen aid (stainless-steel melon round baller) (Lagostina Co., Italy). The average initial mass of each DSG sphere was 4.66 ± 0.05 g, with a diameter of 20.0 ± 0.2 mm. Major, intermediate and minor axes were measured using an image analysis method, and these measurements were used in calculations of the volume of each sample. Over the course of drying, these samples were removed periodically and weighed on an electronic analytical balance (SartoriusB 120 S, Goettingen, Germany) with the accuracy of ± 0.01g. Each of these measurements took only a few seconds, therefore, this time was considered to be insignificant when compared with the overall drying time. Digitized images of the DSG samples were obtained from the top and the side view using an imaging system consisting of a digital camera (Canon Power shot G9), a PC, and a mirror of a 40×100 mm in size (Fig. 1). The digital images were processed with a software package analysis Image J1.29X (National Institutes of Health, USA). To extract a DSG sample contours from the images, an image processing algorithm for noise reduction and segmentation was developed. The conversion of an RGB image into 8-bit grayscale image containing the only blue component of the original view was employed. A 3 x 3 median filter was employed to reduce possible noises within the DSG image. Since the DSG sample was resting on a contrasting black background, the binary process through manual threshold could efficiently distinguish DSG contours from the remaining part of image with an optimal value. The grey level histogram of the image had clear peaks, and the optimal threshold of 153 was easily located by the user. The straight – line selection

tool and wand tool was used to measure three characteristic dimensions of a DSG sample (major, intermediate, and minor axes). The major and the intermediate axes of oblate ellipsoidal geometric form of an object were extracted from the image taken from the top and the minor axis was extracted from the mirror image. Each test included eight spheres and was repeated four times for a single element.

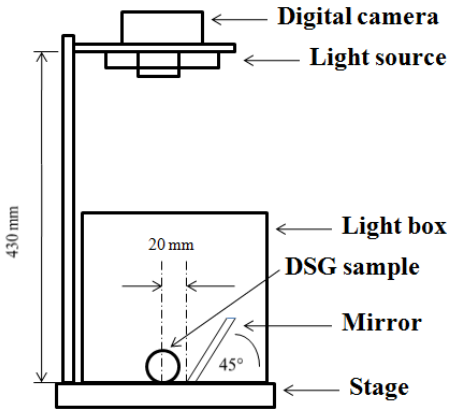

Fig. 1. A set up for imaging a sample size

Calibration tests were performed to determine the scaling factor between the real size of an object and the size of the same object reflected in the 45° mirror. The determined scaling factor was 1.14. Also, the image system was calibrated against two Teflon spheres of 9.65 and 8.08 mm diameter. The difference between the true volume of the spheres determined based on dimensions measured with a micrometer and with the digitized images were less than 1%.

Statistical analysis Data were analyzed using Statistica 8.0 (StatSoft Inc., Tulsa, OK) software. The data were subjected to a one factor analysis of variance. The significance of differences was determined by the Duncan multiple range test at $p \leq 0.05$. The constants of models were determined using a non-linear regression procedure based on the Levenberg–Marquardt algorithm. The concordance between experimental and calculating data was determined by the coefficient of determination (R^2).

RESULTS The initial moisture content of the solid fraction of DSG used for the drying experiments was 2.98 ± 0.08 d.b. (dry basis). Drying curves of the moisture content and temperature changes as a function of time for DSG dried in 110, 130 and 160°C SS and velocity of 1.0 m/s are shown in Fig. 2. A significant increase of drying rate was observed due to SS temperature changes from 110 to 160°C. Experimental data for moisture content changes show that DSG gained moisture at the beginning of drying due to steam condensation on the material surface. A rapid increase in material temperature was observed until the temperature of the product attained the saturation temperature. Then, a constant rate period followed by a single falling rate period was observed. The first drying rate period occurred past the saturation point, when the moisture gained on the surface of the material due to steam condensation (acting as free water) evaporated under 100°C. During this period, the heat transferred to the material was used only to evaporate the free water that condensed on the material surface. The material temperature remained constant until free water disappeared from the material's surface. The falling drying rate period was observed, when the temperature of DSG began increasing while moisture changes were following an exponential curve and eventually reaching a plateau. Drying curves and drying rates were used for the determination of constant and falling rate periods.. The experimental point that corresponds to the critical moisture content (MC_{cr}) is 1.05 ± 0.23 (d.b.) depending on the SS temperature applied during drying.

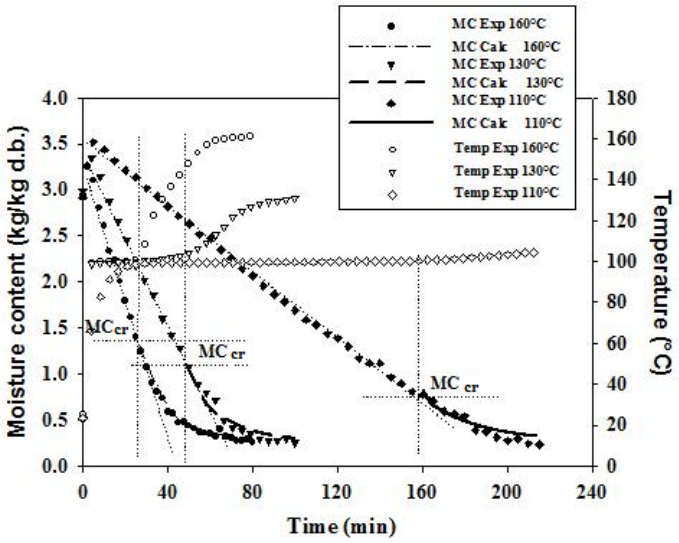

Fig. 2. Experimental data of moisture content and material temperature changes during drying. Validation of the simulation results of Eq. (1) against measured data points for moisture changes of DSG sample during drying in SS at temperature 110, 130, 160°C and velocity 1.0 m/s. The simulation was done assuming no shrinkage of a sample took place. (Abbreviation meanings: exp - experimental data, calc - calculated data).

The observed falling rate period was described with the Fick's second law of diffusion. The validation of the simulation results of Eq. (1) against measured data points for moisture changes of DSG sample predicted based on non-shrinkage conditions is shown in Fig. 2. The validation was conducted for SS drying at temperature 110, 130, 160°C and velocity 1.0 m/s. The values of the determination coefficient (R^2) were: 0.8285, 0.9031 and 0.9674 at SS temperature 110, 130, 160°C, respectively. For the case of non-shrinkage the values of the moisture content in DSG predicted from the Eq. (1) were overestimated at the final drying phase.

The use of the image system to measure changes in volume of the DSG layer on inert particle was not suitable owing to the nature of the samples investigated in this study. During the course of drying, the material deformed easily creating openings within the material structure and producing empty spaces between DSG layer and inert particle. As long as the volume shrinkage was considered, and the assumptions of uniform structure and uniform shrinkage in all dimensions of the material were given, it was still in accordance with the general rules, to measure the changes in volume of sphere instead of thin-layer of material compressed over the surface of a solid sphere (Fig. 3).

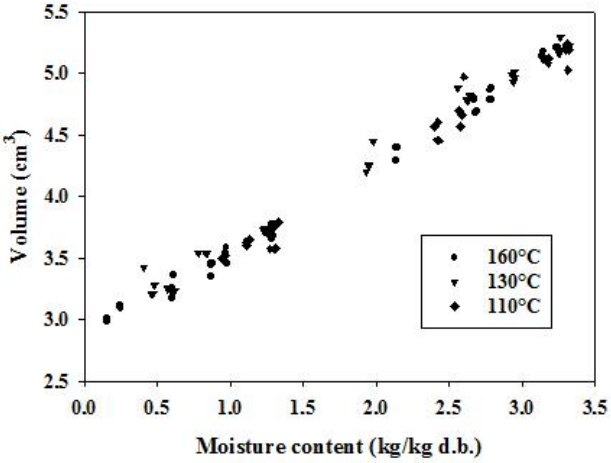

Fig. 3. Changes in volume of DSG during drying at SS temperature 110, 130, 160°C and velocity 1.0 m/s.

The linear Eq. (6) was used to describe the dimensionless volume change with respect to moisture. Coefficients A and B were determined for DSG for the SS temperature range of 110 - 160°C, which did not show any significant effect on shrinkage in the tested range (Zielinska & Markowski, 2007). Thus, the relationship between the dimensionless volume and moisture for DSG is:

$$\frac{V}{V_0} = 0.7188\frac{M}{M_0} + 2.8644 \tag{7}$$

Fig. 4 shows the effect of the diffusivity coefficient and shrinkage on the accuracy of the prediction of drying characteristic. The measured data points (symbols) are compared against the three simulation lines (1, 2, 3). Line 1 simulates drying kinetics when the coefficient of diffusivity was determined assuming no-shrinkage. Line 2 shows the effect of incorporating shrinkage by recalculating the thickness of the dried layer but using the diffusivity coefficient determined for non-shrinkage conditions. For the second case, the changes in the moisture were underpredicted (Fig. 4, line 2). The diffusivity coefficient was adjusted for the best fit to the experimental data (line 3), and the simulation was conducted incorporating the effect of the shrinkage. The validation of simulation results of Eq. (1) shows that neglecting the shrinkage phenomena during modeling drying kinetics leads to different results on moisture changes during drying.

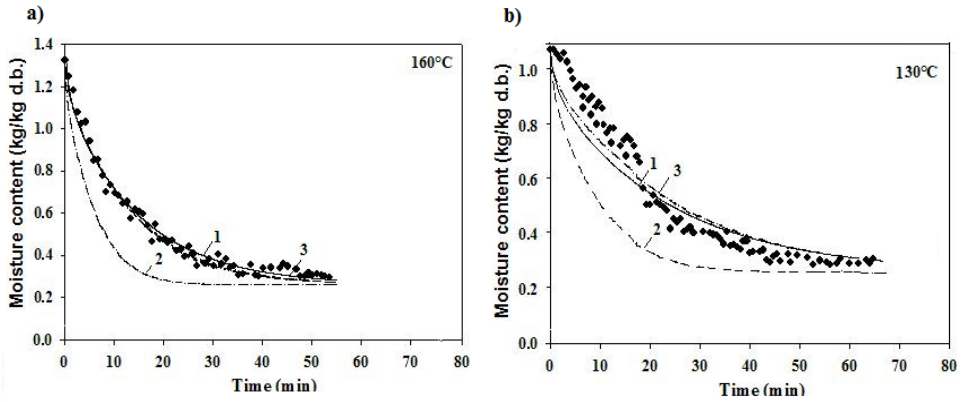

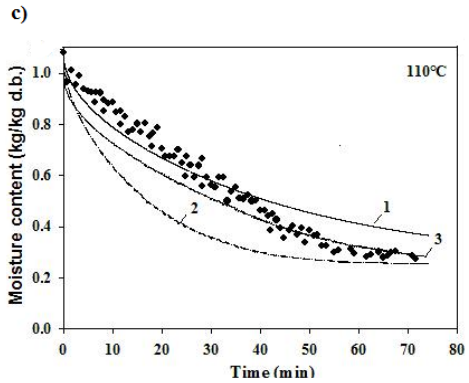

Fig. 4. Simulation results of DSG drying in three different SS temperatures: a) 110; b) 130; c) 110°C showing the sensitivity of the diffusion coefficient to shrinkage. Symbols – experimental data, line 1 - the simulation conducted at the diffusivity determined with no shrinkage, line 2 - the simulation conducted when change in the layer thickness was due to shrinkage and the diffusivity determined based on the non-shrinkage condition, line 3 - the simulation conducted with the shrinkage conditions and the diffusivity determined for the best fit to the experimental data points.

Table 1. Mean values and standard errors of the means for the coefficients in Eq. (4), when drying DSG in SS at temperatures of 110, 130, 160°C and velocity 1.0 m/s.

Coefficients of Eq. (4)	Non-shrinkage				Shrinkage	
	1*		2*		3*	
	Mean	SEM	Mean	SEM	Mean	SEM
D_0 (m^2/s)	2.27×10^{-8}	0.11×10^{-8}	3.62×10^{-4}	0.21×10^{-4}	2.46×10^{-8}	0.11×10^{-8}
k_T (1/K)	1.03×10^{3}	0.06×10^{3}	3.78×10^{3}	0.12×10^{3}	1.49×10^{3}	0.09×10^{3}
k_M (kg/kg)	2.06×10^{-1}	0.03×10^{-1}	1.50×10^{1}	0.08×10^{1}	3.38×10^{-1}	0.06×10^{-1}
R^2	0.8876		0.8894		0.9666	

SEM - Standard error of the mean
1* the simulation conducted at the diffusivity determined with no shrinkage
2* the simulation conducted when change in the layer thickness was due to shrinkage and the diffusivity determined based on non-shrinkage conditions
3* the simulation conducted with shrinkage conditions and the diffusivity determined for the best fit conditions to the experimental data points

The effective moisture diffusivity for DSG during SS drying as a function of moisture content and temperature was calculated from Eq. (4). The results of the parameter estimations in Eq. (4) are shown in Table 1. Assuming shrinkage or non-shrinkage conditions showed that the model parameters are sensitive to temperature and moisture content changes. The value of parameter D_0 was the highest (3.62×10^{-4} m/s^2)in comparison to the other two cases.

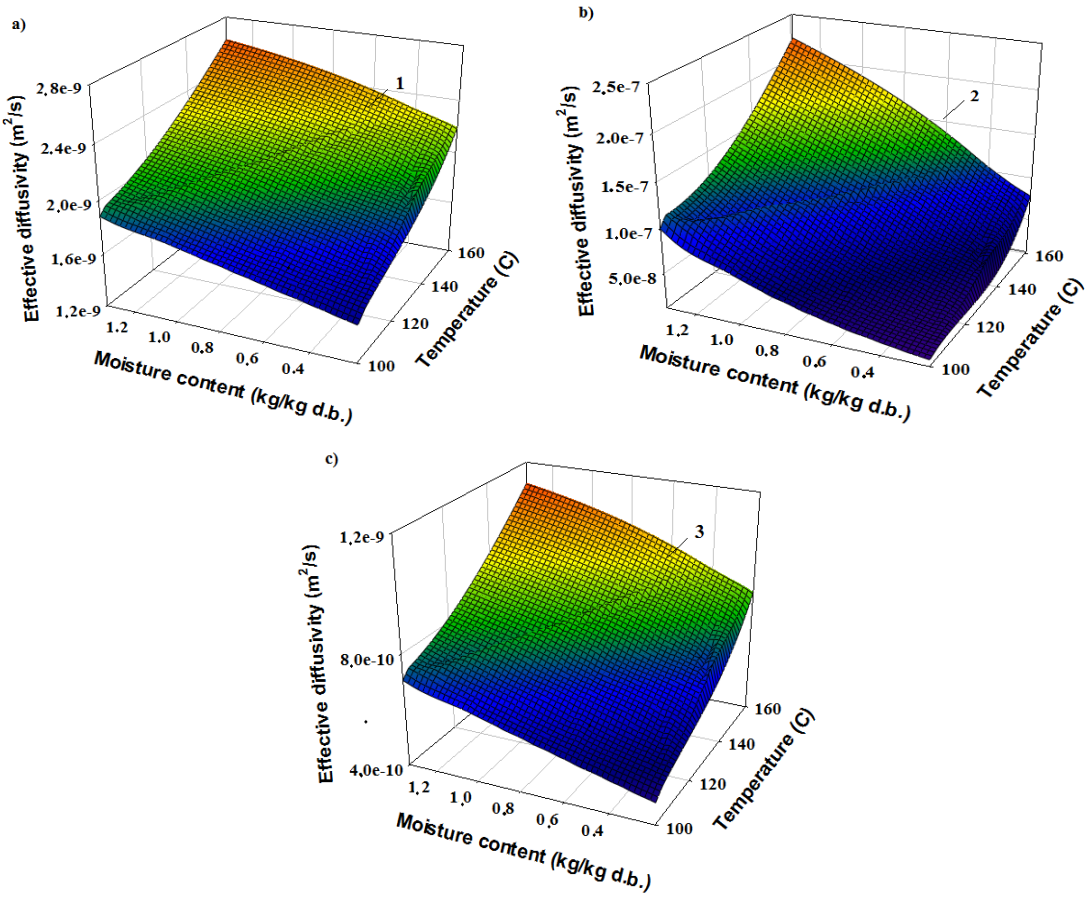

Fig. 5. Effective moisture diffusivity of DSG as affected by moisture content and temperature of material for SS drying at temperature 110, 130, 160°C and velocity 1.0 m/s. Simulations conducted for a) the diffusivity determined considering no shrinkage (mesh 1), b) changes in the layer thickness considered but the diffusivity determined for non-shrinkage (mesh 2); c) shrinkage conditions and the diffusivity determined from the best fit (mesh 3).

Fig. 5 shows the simulation results of the effect of moisture content and the material temperature on the effective moisture diffusivity of DSG. Mesh 1 represents the simulation conducted when the change in the layer thickness was neglected and the diffusivity was determined with the non-shrinkage condition. Mesh 2 shows the simulation that was conducted with the assumption that the change in the DSG layer thickness (Eq. 1) was due to shrinkage and the diffusivity was determined based on the non-shrinkage condition. Mesh 3 represents the simulation conducted with the shrinkage condition and the effective diffusivity determined for the best fit to the experimental data.

The values of the effective moisture diffusivity calculated from the Eq. (1) assuming no-shrinkage took place ranged between 1.45×10^{-9} and 2.21×10^{-9} m^2/s. The values of effective moisture diffusivity ranged between $1.04\times10^{-7}$and 2.13×10^{-8} m^2/s when the change in the layer thickness was caused by the shrinkage but the diffusivity determined for non-shrinkage. The path of moisture diffusion inside the dried material when shrinkage was not considered was longer than the one when change in the layer thickness was due to shrinkage. Therefore, the simulation was also conducted considering the change in the layer thickness due to shrinkage and determining the effective diffusivity

for the best fit to the experimental data (mesh 3). Simulation results show that shrinkage of DSG during drying should be taken into account to attain reliable values of effective moisture diffusivity. The calculated diffusion coefficient was the highest for the non-shrinkage assumption. The results of the simulation considering the shrinkage and the diffusivity adjusted for the best fit to the experimental data gave the values of the effective diffusivity lower by 60% ranging from 5.08×10^{-10} to 8.24×10^{-10} m^2/s.

CONCLUSIONS Three simulations of drying of DSG in superheated steam at different assumptions re shrinkage led to the following conclusions: Neglecting shrinkage of DSG, the determined effective moisture diffusivity ranged between 1.45×10^{-9} and 2.21×10^{-9} m^2/s. The values of the effective moisture diffusivities varied from 3.02×10^{-8} to 5.28×10^{-8} m^2/s when the change in the layer thickness due to the shrinkage was considered but the diffusivity determined based on the non-shrinkage condition. The effective diffusivity coefficient determined for the best fit condition to the experimental data ranged between 5.08×10^{-10} to 8.24×10^{-10} m^2/s. Neglecting the shrinkage phenomena during drying overestimated the values of the moisture diffusivity of DSG.

Acknowledgements The study was financially supported by the Polish Ministry of Science and Higher Education through the program entitled ‘‘Supporting International Mobility of Researchers’’. Also, partial funding was provided by the Natural Sciences and Engineering Research Council of Canada (NSERC).

REFERENCES

Benali, M., M. Amazouz. 2006. Drying of vegetable starch solutions on inert particles: Quality and energy aspects. Journal of Food Engineering, 74, 484–489.

Crank, J. The Mathematics of Diffusion, Oxford University Press, Oxford, 1975.

Kudra, T., A.S. Mujumdar. Advanced drying technologies. NY: Marcel Dekker Inc., 2002.

Mohsenin, N.N. Physical Properties of Plant and Animal Materials. Gordon and Breach Publishers, NY, 1986.

Mulet, A. 1994. Drying Modeling and Water Diffusivity in Carrots and Potatoes, Journal of Food Engineering, 22, 329–348.

Pabis, S., D.S. Jayas, S. Cenkowski. Grain Drying: Theory and Practice. John Wiley and Sons; NY, 1998.

Reyes, A., P.I. Alvarez, F.H. Marquardt. 2002. Drying of Carrots in a Fluidized Bed. I. Effects of Drying Conditions and Modelling. Drying Technology, 20(7), 1463-1483.

Zielinska, M., S. Cenkowski. 2009. Comparison of Drying Kinetics of Spent Grain Dried on Inert Material of Different Heat Capacity. *CSBE/SCGAB,* 2009. Prince Edward Island, July 12-15, 2009, (23p).

Zielinska, M., S. Cenkowski, M. Markowski. 2009. Superheated Steam Drying of Distillers' Spent Grains on a Single Inert Particle. Drying Technology. An International Journal, 27, 12, 1279-1285.

Zielinska, M., M. Markowski. 2007. Drying Behavior of Carrots Dried in a Spout-Fluidized Bed Dryer. Drying Technology, 25, 261–270.

Zielinska, M., M. Markowski. 2010. Air drying characteristics and moisture diffusivity of carrots, Chem. Eng. Process. doi:10.1016/j.cep.2009.12.005